Experimental Realization of a Quantum Spin Pump

Susan K. Watson,[1,2] R. M. Potok,[2] C. M. Marcus,[2] and V. Umansky[3]
[1]*Department of Physics, Middlebury College, Middlebury, Vermont 05753, USA*
[2]*Department of Physics, Harvard University, Cambridge, Massachusetts 02138, USA*
[3]*Braun Center for Submicron Research, Weizmann Institute of Science, Rehovot 76100, Israel*
(Received 1 June 2003; published 18 December 2003)

We demonstrate the operation of a quantum spin pump based on cyclic radio-frequency excitation of a GaAs quantum dot, including the ability to pump pure spin without pumping charge. The device takes advantage of bidirectional mesoscopic fluctuations of pumped current, made spin dependent by the application of an in-plane Zeeman field. Spin currents are measured by placing the pump in a focusing geometry with a spin-selective collector.

DOI: 10.1103/PhysRevLett.91.258301 PACS numbers: 85.75.–d, 72.25.–b

Using electron spin to encode information in semiconductors holds promise for integrating computation and storage [1] and, in coherent systems, is expected to provide significantly increased immunity from environmental decoherence compared with conventional charge-based electronics [1,2]. Among the needed elements for any spin-based electronic system is a device that generates a spin current, the analog of a battery in conventional electronics. Candidates for such devices include injection schemes based on magnetic semiconductors [3,4] and ferromagnetic metals [5,6], ferromagnetic resonance devices [7], and a variety of spin-dependent pumps [8–14].

In this Letter, we demonstrate the operation of such a quantum-dot-based spin pump — including the ability to pump pure spin without pumping charge — using a gate-defined lateral quantum dot fabricated on a GaAs/AlGaAs heterostructure. Pumping of charge using cyclic gate voltages applied to a phase-coherent dot has been the subject of numerous investigations (mostly theoretical) in the past several years [15–20]. Quantum pumps are closely related to classical charge pumps using Coulomb blockade [21,22] as well as higher-frequency mesoscopic photovoltaic effects [20,23–25] and photon-assisted tunneling [26]. A recent proposal by Mucciolo, Chamon, and Marcus (MCM) [8] considered a quantum-dot-based charge pump in the presence of sizable Zeeman splitting, and showed that such a device would function as a phase-coherent spin pump. An important feature of the MCM proposal is that it remains operational regardless of whether the pumped current arises from adiabatic pumping [15–18,20], mesoscopic rectification [18,27,28], or photovoltaic mechanisms [20,23] as long as the fluctuations of pumped current are larger than the average, so that both positive and negative current can be generated and controlled by external parameters such as device shape or applied magnetic flux.

In order to realize the spin pump device experimentally, radio-frequency (rf) sinusoidal voltages were applied to two shape-defining gates of a quantum dot, producing a dc current through the quantum dot due to a combination of adiabatic pumping and rectification effects. As discussed in detail below, while pumped charge can be measured directly across the device, measuring the pumped *spin* is more subtle, and in the present setup is detected using an electron focusing configuration with a quantum point contact operating as a spin detector [29,30].

Because of quantum coherence, the direction of the pumped current is a mesoscopically fluctuating quantity with zero average. In the absence of an external magnetic field, $B_{\|} = 0$, the two spin states are degenerate and the pumped currents for spin-up ($I_\uparrow$) and spin-down ($I_\downarrow$) are identical, fluctuating together as control parameters are swept (this is also the case for mesoscopic rectification [28]). In this zero-field case, pumping induces a net charge current $I_c = I_\uparrow + I_\downarrow \neq 0$, but no net spin current, $I_s = I_\uparrow - I_\downarrow = 0$, as illustrated schematically in Fig. 1(a). For sufficiently strong in-plane magnetic fields, $g\mu_B B_{\|} > (kT, \Gamma)$, spin-up and spin-down pumped currents are uncorrelated. Here, Γ is the level broadening due to escape and dephasing, $g \sim -0.4$ is the electron g factor, and μ_B is the Bohr magneton. In this high-field case, pumped charge is composed of independent contributions of $I_\uparrow$ and

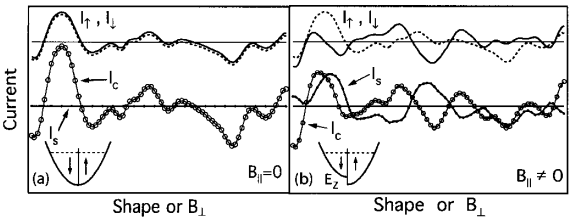

FIG. 1. Schematic illustration of how mesoscopic pumping fluctuations plus Zeeman splitting can give rise to independent fluctuations of charge current $I_c = I_\uparrow + I_\downarrow$ and spin current $I_s = I_\uparrow - I_\downarrow$, based on Ref. [8]. (a) At $B_{\|} = 0$ one has $I_\uparrow = I_\downarrow$; hence $I_s = 0$. (b) At large in-plane fields, $B_{\|} > (kT, \Gamma)$ (see text), spin degeneracy is lifted, $I_\uparrow$ is uncorrelated with $I_\downarrow$, and in general $I_s \neq 0$. In this case, one may even have a pure spin pump when $I_s \neq 0$ while $I_c = 0$.

$I_\downarrow$ [Fig. 1(b)], and in general a nonzero spin current exists. In practice, it is straightforward in this regime to tune the charge current to zero (using a gate-defined dot shape or a small applied perpendicular magnetic flux) resulting in a *pure spin current.*

To detect the presence of a spin current, we take advantage of a spin-sensitive electron focusing geometry (Fig. 2, inset), which allows the pumped current to be focused into a collector quantum point contact (QPC), as shown in Fig. 2. In moderate in-plane fields, $B_\parallel \gtrsim 3$ T, the collector QPC has been shown to act as a spin-sensitive detector whenever its conductance g_c is tuned (by gate voltages) to $g_c \leq 1e^2/h$ [29,30]. In this spin-sensitive regime, the base-collector voltage reflects the polarization of the current impinging upon the collector QPC. As a control, when the collector QPC is non-spin-sensitive, which is achieved — even in high fields — by setting $g_c = 2e^2/h$, the base-collector voltage signal reflects the total charge current impinging on the collector QPC.

The complete system, comprising the quantum-dot spin pump plus the QPC-focusing test structure, was fabricated on a GaAs/AlGaAs two-dimensional electron gas using *e*-beam patterned CrAu depletion gates and nonmagnetic (PtAuGe) Ohmic contacts. The high-mobility material ($\mu = 5.5 \times 10^6$ cm^2 V^{-1} s^{-1}) was useful for obtaining good focusing but is not necessary for the operation of the spin pump itself. This mobility, and sheet density $n = 1.3 \times 10^{11}$ cm^{-2}, gave a mean-free path of 45 μm. The quantum dot, which has an area of $A \sim 0.1$ μm^2, is typically operated with one fully open channel in each of its point contact leads, $g_{\text{lead1}} \sim g_{\text{lead2}} \sim 2e^2/h$.

Focusing was first tested and calibrated using a current-bias configuration ($I_{\text{bias}} = 1$ nA). Results are shown in Fig. 2. Next, two sinusoidal signals at 10 MHz with controllable phase difference, ϕ, were applied (via synchronized Agilent 33250 synthesizers) to two of the confining gates of the dot: $V_{\text{gate1}}(t) = V_{\text{dc1}} + V_1 \sin(\omega t)$, $V_{\text{gate2}}(t) = V_{\text{dc2}} + V_2 \sin(\omega t + \phi)$. Applying ac gate voltages of 70 mV (comparable to the characteristic gate-voltage scale of gate-induced mesoscopic conductance or pumping fluctuations (see Fig. 3) induced a dc current through the dot on the scale of ~10–100 pA, measured using an Ithaco 1211 current amplifier with input

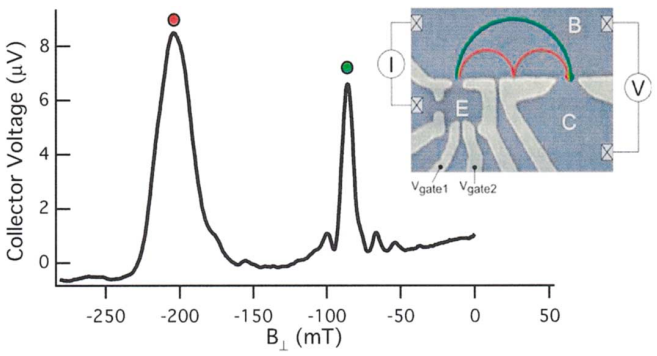

FIG. 2 (color). The base-collector voltage as a function of perpendicular magnetic field, $B_\perp$. The first (green dot) and second (red dot) focusing peaks in the base-collector voltage occur when the spacing between the emitter (quantum dot) and the collector (QPC) is a multiple of the cyclotron diameter. To find the focusing peaks, a current bias of 1 nA was applied across the dot. Inset: Electron micrograph of the dot/focusing device, with added circuit and schematic trajectories. Electrons emitted from the quantum dot emitter, "E," follow ballistic trajectories through the base region, "B," into the collector, "C." The ac voltages V_{gate1} and V_{gate2} are applied to shape-defining gates.

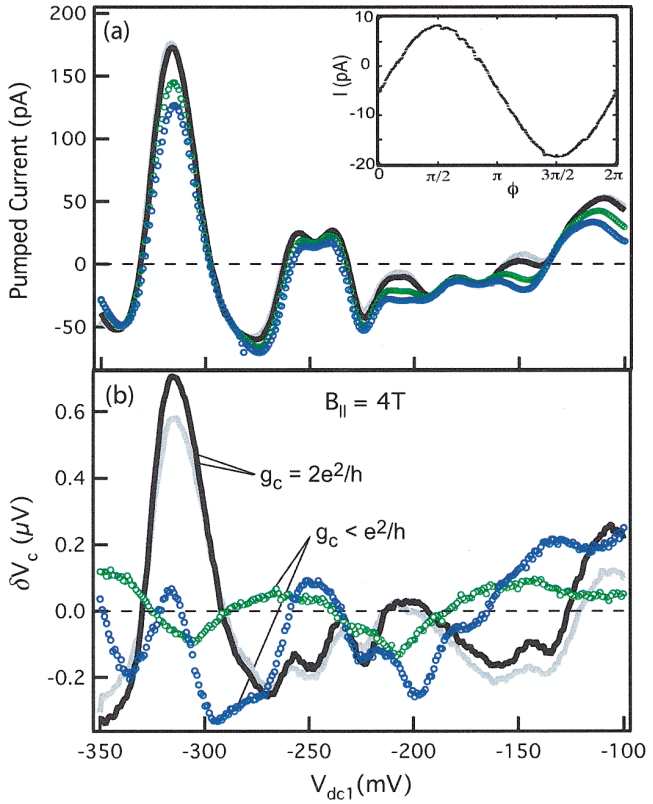

FIG. 3 (color). (a) The pumped charge current at $B_\parallel = 4$ T and $\phi = 3\pi/2$ as a function of dot shape, controlled by dc gate voltage V_{dc1}. Traces at slightly different collector QPC settings, both with $g_c = 1e^2/h$ (gray and black) are similar, and are also similar to the traces with $g_c \leq 1e^2/h$ (green and blue). Inset: Pumped current as a function of the phase ϕ between V_{gate1} and V_{gate2}. (b) Collector voltages (measured relative to the base region), $\delta V_c = V_c - \langle V_c \rangle$, on the second focusing peak under the same conditions as corresponding traces in (a) [31,32]. For spin-insensitive collector QPC, $g_c \sim 2e^2/h$ (gray and black), collector voltages track pumped current, indicating that the voltage measures the total charge current. For spin-selective collector QPC, $g_c \leq 1e^2/h$ (green and blue), the collector voltages are uncorrelated with pumped current and from traces at $g_c \sim 2e^2/h$.

impedance ~20 Ω (much lower than the Ohmic contact resistance of ~1 kΩ). The rf applied to the gates was modulated at 11 Hz to allow lock-in detection of both the pumped current, measured through the base-emitter circuit, and the voltage across the collector QPC.

The sinusoidal dependence of pumped current on ϕ, $I(\phi) \sim I_o \sin(\phi)$ [Fig. 3(a), inset] is consistent with both adiabatic quantum pumping [17,19] and capacitively coupled rectification [28]. However, the fact that the magnitude of current is typically larger than 1 electron per cycle (= 1.6 pA at 10 MHz) suggests that the pumped current is dominated by rectification rather than adiabatic pumping. Again, this does not affect the performance of the spin pump.

Figure 3 shows pumped current and collector voltages at $B_\parallel = 4$ T for both spin-selective and nonselective settings of the collector QPC, as a function of dc voltage on one of the shape-defining gates of the quantum dot. The point contacts of the dot were each set at $2e^2/h$, the pumping amplitude was $V_1 = V_2 = 70$ mV, and the phase was $\phi = 3\pi/2$. A linear background signal due to rectification has been subtracted from the collector voltage data in Fig. 3(b), $\delta V_c = V_c - \langle V_c \rangle$, where V_c is the collector voltage and $\langle V_c \rangle$ is its average over the trace [32].

The data in Fig. 3 illustrate our main experimental observation: when the collector QPC is set to $g_c = 2e^2/h$, and hence is *not* spin selective, the collector voltage closely follows the pumped current. In contrast, when the collector QPC is spin selective, $g_c \leq 1e^2/h$, the collector voltage appears unrelated to the pumped total charge current. Moreover, small changes to the collector gate voltage in the spin-selective region, $g_c \leq 1e^2/h$, produce different degrees of spin filtering giving collector voltages with uncorrelated mesoscopic fluctuations (Fig. 3, blue and green circles). The observation that the collector voltage on a focusing peak is uncorrelated with total current *only when the collector point contact is spin selective* indicates that a spin current —*fluctuating independently from the total current* — is being generated by the pump.

One may readily identify in Fig. 3 several zeros of the total current. At these points, the pump operates as a pure spin pump, producing tens of spins per cycle, with zero net charge being pumped. At these points, spin-up and spin-down currents are pumped in opposite directions, producing zero net charge current through the dot, but a nonzero spin current measured by the spin-sensitive collector QPC.

The corresponding control experiment, shown in Fig. 4, demonstrates that at $B_\parallel = 0$ collector voltages show essentially identical fluctuation patterns regardless of the collector QPC setting. This behavior is expected when the quantum-dot pump produces no spin polarized current and the collector is not spin sensitive. In this case, the collector voltage simply reflects the total pumped current.

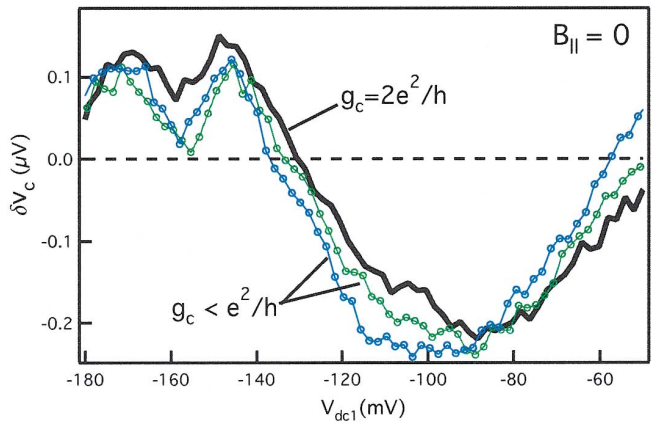

FIG. 4 (color). Collector voltage as a function of dot shape for $B_\parallel = 0$ at two different collector QPC settings, with $g_c \leq 1e^2/h$ and $g_c \sim 2e^2/h$ [31,32]. Unlike the situation at $B_\parallel = 4$ T, the collector voltage is not sensitive to the conductance of the collector QPC. This is anticipated as there is no spin selectivity of the collector QPC nor is there a pumped spin current from the dot.

In summary, we have demonstrated a mesoscopic spin pump using an ac driven phase-coherent quantum dot in a Zeeman field. Spin current — including pure spin current, without any charge current — is detected using a spin-sensitive focusing technique [29,30]. While this experiment required the application of a sizable in-plane magnetic field, one can expect similar results using permanent magnets microfabricated along with the quantum dot. This would be particularly effective in materials with a larger g factor than GaAs. It is of interest to clarify how spin-orbit coupling affects the operation of the pump [13]. We speculate that in strong spin-orbit materials it may be sufficient to break time-reversal symmetry with a small applied field (on the scale of a few flux quanta through the dot, typically of order 0.01 T for a square-micron dot area). These interesting extensions await further experimental investigation.

We thank Joshua Folk for valuable discussions and assistance in carrying out the measurements, and Piet Brouwer for useful discussions. Research at Harvard was supported by the DARPA-SpinS program and the National Science Foundation under DMR 0072777. R. P. acknowledges support from the Army Research Office under QuaCGR Program. S. W. acknowledges support from Middlebury College and the National Science Foundation (DMR-0074930).

[1] S. A. Wolf, D. D. Awschalom, R. A. Buhrman, J. M. Daughton, S. von Molnar, M. L. Roukes, A. Y. Chtchelkanova, and D. M. Treger, Science **294**, 1488 (2001).

[2] *Semiconductor Spintronics and Quantum Computation*, edited by D. Awschalom, N. Samarth, and D. Loss (Springer, New York, 2002).
[3] R. Fiederling, M. Keim, G. Reuscher, W. Ossau, G. Schmidt, A. Waag, and L.W. Molenkamp, Nature (London) **402**, 787 (1999).
[4] Y. Ohno, D. K. Young, B. Beschoten, F. Matsukura, H. Ohno, and D. D. Awschalom, Nature (London) **402**, 790 (1999).
[5] W. Y. Lee, S. Gardelis, B. C. Choi, Y. B. Xu, C. G. Smith, C. H.W. Barnes, D. A. Ritchie, E. H. Linfield, and J. A. C. Bland, J. Appl. Phys. **85**, 6682 (1999); P. R. Hammar, B. R. Bennett, M. J. Yang, and M. Johnson, Phys. Rev. Lett. **83**, 203 (1999).
[6] H. J. Zhu, M. Ramsteiner, H. Kostial, M. Wassermeier, H. P. Schonherr, and K. H. Ploog, Phys. Rev. Lett. **87**, 016601 (2001).
[7] A. Brataas, Y. Tserkovnyak, and G. E.W. Bauer, Phys. Rev. B **66**, 060404 (2002); Y. Tserkovnyak, A. Brataas, and W. E.W. Bauer, Phys. Rev. B **66**, 224403 (2002).
[8] E. R. Mucciolo, C. Chamon, and C. Marcus, Phys. Rev. Lett. **89**, 146802 (2002).
[9] Junling Wu, Baigeng Wang, and Jian Wang, Phys. Rev. B **66**, 205327 (2002).
[10] T. Aono, Phys. Rev. B **67**, 155303 (2003).
[11] Wei Zheng, Junling Wu, Baigeng Wang, Jian Wang, Qingfeng Sun, and Hong Guo, e-print cond-mat/0211460.
[12] P. Sharma and C. Chamon, Phys. Rev. Lett. **87**, 096401 (2001).
[13] M. Governale, F. Taddei, and R. Fazio, e-print cond-mat/0211211.
[14] Martin J. Stevens, Arthur L. Smirl, R. D. R. Bhat, Ali Najmaie, J. E. Sipe, and H. M. van Driel, Phys. Rev. Lett. **90**, 136603 (2003).
[15] B. Spivak, F. Zhou, and M. T. B. Monod, Phys. Rev. B **51**, 13 226 (1995).
[16] F. Zhou, B. Spivak, and B. Altshuler, Phys. Rev. Lett. **82**, 608 (1999).
[17] P.W. Brouwer, Phys. Rev. B **58**, 10135 (1998).
[18] M. Switkes, C. M. Marcus, K. Campman, and A. C. Gossard, Science **283**, 1905 (1999).
[19] T. A. Shutenko, I. L. Aleiner, and B. L. Altshuler, Phys. Rev. B **61**, 10366 (2000).
[20] M. G. Vavilov, V. Ambegaokar, and I. L. Aleiner, Phys. Rev. B **63**, 195313 (2001).
[21] H. Pothier, P. Lafarge, C. Urbina, D. Esteve, and M. H. Devoret, Europhys. Lett. **17**, 249 (1992).
[22] L. P. Kouwenhoven, A. T. Johnson, N. C. van der Vaart, C. J. P. M. Harmans, and C. T. Foxon, Phys. Rev. Lett. **67**, 1626 (1991).
[23] V. I. Fal'ko, Europhys. Lett. **8**, 785 (1989).
[24] A. A. Bykov, G. M. Gusev, Z. D. Kvon, D. I. Lubyshev, and V. P. Migal, JETP Lett. **49**, 13 (1989).
[25] L. DiCarlo, C. M. Marcus, and J. S. Harris, Jr., e-print cond-mat/0304397.
[26] L. P Kouwenhoven, S. Jauhar, J. Orenstein, P. L. McEuen, Y. Nagamune, J. Motohisa, and H. Sakaki, Phys. Rev. Lett. **73**, 3443 (1994).
[27] H. Linke, W. Sheng, A. Lofgren, H. Q. Xu, P. Omling, and P. E. Lindelof, Europhys. Lett. **44**, 341 (1998); H. Linke, T. E. Humphrey, A. Lofgren, A. O. Sushkov, R. Newbury, R. P. Taylor, and P. Omling, Science **286**, 2314 (1999).
[28] P.W. Brouwer, Phys. Rev. B **63**, 121303 (2001).
[29] R. M. Potok, J. A. Folk, C. M. Marcus, and V. Umansky, Phys. Rev. Lett. **89**, 266602 (2002).
[30] J. A. Folk, R. M. Potok, C. M. Marcus, and V. Umansky, Science **299**, 679 (2003).
[31] Cross coupling between the collector QPC voltage and the gates of the emitter dot causes current and voltage curves Figs. 3 and 4 to shift small amounts horizontally ($<$20 mV). The current traces are easily brought into alignment with small horizontal shifts, done by eye; the corresponding collector voltage traces are then shifted horizontally by the same amount as their respective current traces.
[32] In this three-terminal geometry, rectification due to rf gate voltages gives rise to dc currents across the dot, with mesoscopic fluctuations as a function of dot shape (as discussed in the text), as well as dc voltages across the collector, which do not depend on dot shape. The later rectification effect gives rise to a nonzero $\langle V_c \rangle$ that varies with collector gate-voltage settings but does not depend on the dot gate voltages. Note that this offset, removed in Figs. 3 and 4 by shifting collector voltages vertically, does not affect correlations between collector voltages as a function of dot shape at different settings of g_c, or correlations between pumped current and collector voltage.